Journal of Magnetism and Magnetic Materials 378 (2015) 278–284

Contents lists available at ScienceDirect

Journal of Magnetism and Magnetic Materials

journal homepage: www.elsevier.com/locate/jmmm

Synthesis, characterization and FC–ZFC magnetization studies of cobalt substituted lithium nano ferrites

G. Aravind [a], M. Raghasudha [b], D. Ravinder [a,*]

[a] Department of Physics, Osmania University, Hyderabad 500007, Telangana, India
[b] Department of Chemistry, Jayaprakash Narayan College of Engineering, Mahabubnagar 509001, Telangana, India

ARTICLE INFO

Article history:
Received 11 July 2014
Received in revised form
8 November 2014
Accepted 14 November 2014
Available online 20 November 2014

Keywords:
Citrate-gel auto-combustion technique
Nano ferrites
Magnetic properties
Field cooled (FC)
Zero field cooled (ZFC) Magnetization
Superparamagnetism

ABSTRACT

Cobalt substituted Lithium Nano ferrites with the chemical composition $[Li_{0.5}Fe_{0.5}]_{1-x}Co_xFe_2O_4$ (where $x=0.0, 0.2, 0.4, 0.6, 0.8, 1.0$) were synthesized through Citrate-Gel auto combustion technique. Structural characterization of the prepared ferrites was carried by X-ray diffraction analysis (XRD) and Scanning Electron Microscopy (SEM). XRD analysis has confirmed the formation cubic spinel structure of the ferrite compositions with a particle size ranging from 37 nm to 42 nm. The SEM images represent large agglomeration of the nano particles of the ferrite samples with broader grain size distribution. Temperature dependent magnetic properties of $[Li_{0.5}Fe_{0.5}]_{1-x}Co_xFe_2O_4$ for two compositions with cobalt content $x=0.8$ and $x=1.0$ were carried out using Vibrating sample magnetometer (VSM). The magnetization as a function of an applied field ± 10 T was carried out at temperatures 5 K and 310 K. Field cooled (FC) and Zero field cooled (ZFC) magnetization measurements under an applied field of 100 Oe and 1 KOe in the temperature range of 5–375 K were performed. These measurements have resulted the blocking temperature (T_b) at around 350 K i.e. above room temperature for both the ferrites. Below this temperature the ferrites show ferromagnetic behavior and above which superparamagnetic behavior where the coercivity and remanence magnetization are almost zero. Such behavior makes the ferrites to be desirable for biomedical applications.

1. Introduction

In recent years, magnetic nano particles have gained much attention due to their fundamental, technological and scientific importance. Among the various types of magnetic nanoparticles, spinel ferrite nanoparticles are most fascinating materials. The unusual optical, electrical and magnetic properties of ferrite nano particles such as superparamagnetism, low saturation magnetization make the nano-ferrites, a subject of research interest [1]. Properties of spinel ferrites are susceptible to be modified very easily for their wide range of potential applications. This is because, the spinel crystal structure of the ferrites is complex and adaptive, thus can be modified in many ways resulting in novel properties [2].

Lithium ferrite and substituted lithium ferrites have become the candidates of the most attractive materials for microwave applications especially as a replacement for garnets. Their low cost, square hysteresis loop, superior high-temperature performance due to the high Curie temperature are the other prominent properties that make them such promising candidates for microwave devices, for example; isolators, circulators, gyrators and phase shifters [3–4].

Various divalent metal ions such as Co^{2+}, Cd^{2+}, Cu^{2+}, Mg^{2+}, etc. can be used as substituent in lithium ferrites to tailor its properties for device applications. Several investigations on the substitution of different metal ions in lithium ferrites have been carried out and reported to improve the electrical and magnetic properties of lithium ferrite [5–11]. The Co^{2+} being a fast relaxing ion, enhances the microwave properties [12].

Moreover, to the author's knowledge a very little information is available on the low temperature magnetization study of Cobalt substituted lithium ferrites which show the super paramagnetic behavior. This fact motivated the author to study the effect of Co^{2+} on the magnetic properties of the lithium ferrite.

The properties of the spinel ferrites are also dependent on its microstructure, which in turn is sensitive to the method of preparation. Different techniques have been developed for the synthesis of the nano ferrites viz., sol–gel method, micro emulsion, double sintering, hydrothermal, co-precipitation, ball milling and microwave heating to improve the performance of the nano-ferrites [13–16]. Sol–gel auto-combustion is the simple and

* Corresponding author.
E-mail addresses: raghasudha_m@yahoo.co.in (M. Raghasudha), ravindergupta28@rediffmail.com (D. Ravinder).

http://dx.doi.org/10.1016/j.jmmm.2014.11.052
0304-8853/

economic method to synthesize the nanoferrites with good homogeneity at low processing temperature [17]. The present work reports the synthesis, characterization of cobalt substituted lithium ferrites synthesized by Citrate-gel auto combustion method. It also reports FC and ZFC magnetization studies of $[Li_{0.5}Fe_{0.5}]_{1-x}Co_xFe_2O_4$ for two compositions with cobalt content $x=0.8$ and $x=1.0$.

2. Materials and methods

Cobalt substituted Lithium ferrites with the chemical composition $[Li_{0.5}Fe_{0.5}]_{1-x}Co_xFe_2O_4$ where $x=0.0$, 0.2, 0.4, 0.6, 0.8, 1.0 were synthesized through Citrate-Gel auto combustion technique using $LiNO_3$, Co $(NO_3)_2 6H_2O$, Fe $(NO_3)_2 9H_2O$, $C_6H_8O_7 \cdot H_2O$ and NH_3 as starting materials of high purity. Calculated quantities of individual metal nitrates and citric acid were dissolved in double distilled water separately. The stoichiometric calculation during the preparation of the samples gives nominal chemical composition which can be confirmed by Energy Dispersive Spectroscopy measurements. All these solutions were thoroughly mixed together on a magnetic stirrer to result in a citrate nitrate homogeneous solution. Ammonia solution was then added to this solution to adjust its pH to 7. The solution was heated to about 100 °C with constant stirring on magnetic hot plate where all the water molecules were evaporated resulting in the formation of a viscous gel. The gel was continued to heat on the hot plate up to 200 °C. The viscous gel started foaming when all the water molecules were removed from the mixture. The gel has undergone a flame less auto combustion reaction that has started in the hottest portion of the beaker and propagated like a volcanic eruption from the bottom to the top. The reaction has completed just in minute resulting in a loose puffy powder. Finally the burnt ash is subjected to calcination at 500 °C for 4 h in a muffle furnace to obtain spinel

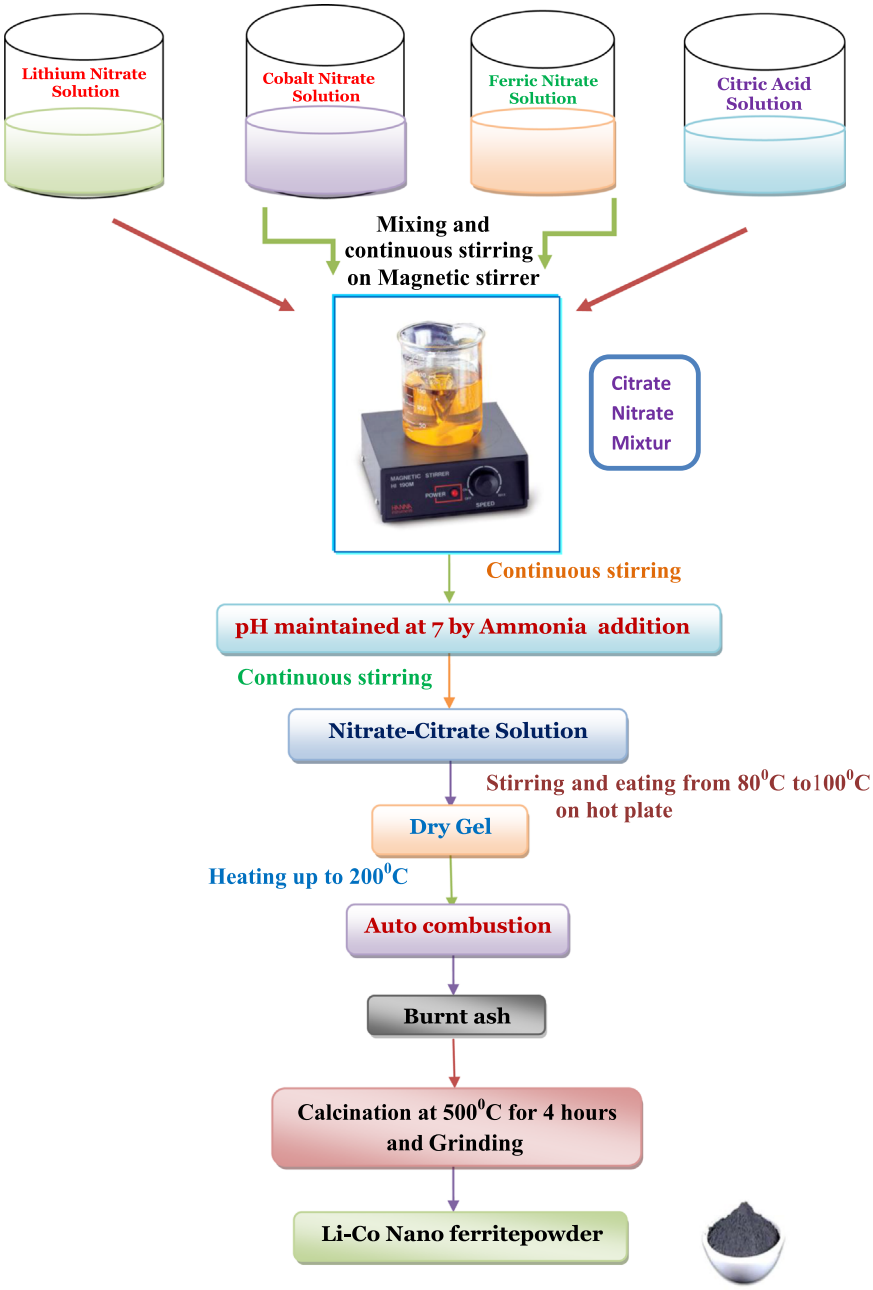

Fig. 1. Flow Chart for the synthesis of Li–Co Nano ferrites.

phase. After calcinations the samples were cooled at a slow rate, as rate of cooling affects the electrical and magnetic properties of the ferrites. Slow cooling results in the formation of ferrites with low particle size, good electrical and magnetic properties. After attaining the room temperature, the samples were taken out off the furnace and ground thoroughly to obtain nano ferrites in spinel phase. The synthesis of Li–Co nano ferrites is shown in Fig. 1 in the form of a flow chart.

3. Characterization

In order to investigate the phase and crystallite size of the synthesized nano ferrites, the structural characterization was performed by X-ray diffractometer (PW3710 Phillips Diffractometer 3710). The experiment was carried out at room temperature by continuous scanning in the range of 2θ°–85θ° using Cu Kα radiation of wave length 1.5405 Å. Structural morphology of the prepared samples was studied by using Scanning Electron Microscope (SEM). Vibrating Sample Magnetometer was used for the ZFC–FC magnetization measurements of two specific ferrite compositions in the temperature range of 5–360 K at different applied fields.

4. Calculation

Using the X-ray diffraction data, the crystallite size of the synthesized samples was calculated using maximum intensity peak from Scherrer's formula [18] as mentioned below

$$\text{Crystallitesize} = D = \frac{0.91\lambda}{\beta Cos\theta} \quad (1)$$

Where λ=the wavelength of X-ray,

β=Full width and half maxima in radians,
θ=Bragg's angle at the peak position.

Lattice parameter 'a' of the individual composition can be calculated using the following expression [18]:

$$a = d\sqrt{h^2 + k^2 + l^2} \quad (2)$$

Where a is lattice parameter, d is inter planar distance, *hkl is* miller indices

The X-ray density (d_x) is calculated using the following relation [18]:

$$x - \text{raydensity} = d_x = \frac{8M}{Na^3}\text{gm/cc} \quad (3)$$

Where M is molecular weight of the sample, N is Avogadro number, a is lattice parameter

Volume of the unit cell 'V' is calculated using the following expression [18]:

$$v = a^3 \quad (4)$$

5. Results and discussion

5.1. XRD analysis

The X-ray diffraction patterns of all the synthesized ferrites were shown in Fig. 2. The diffraction pattern and the crystalline phases were identified in comparison with the standard data from the JCPDS No. 88-0671 of Lithium ferrites. The XRD patterns

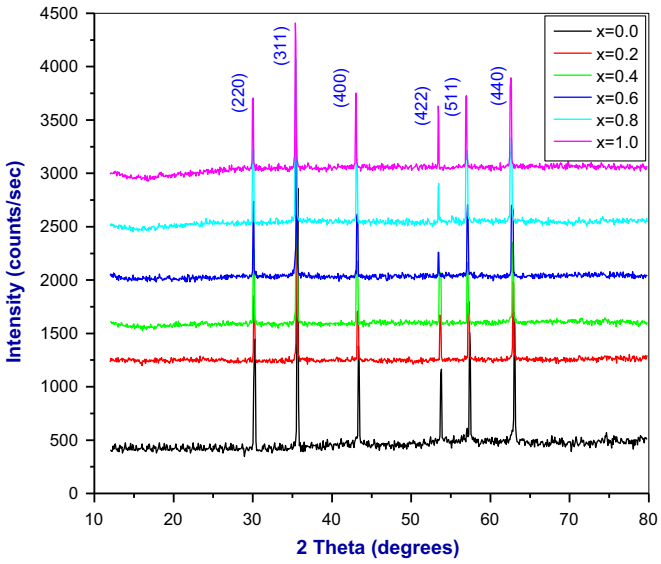

Fig. 2. XRD patterns of $[Li_{0.5}Fe_{0.5}]_{1-x}Co_xFe_2O_4$ where x=0.0, 0.2, 0.4, 0.6, 0.8, 1.0.

indicate formation of well defined peaks of crystalline phase confirming the spinel cubic structure of the samples. All the peaks in the XRD patterns were indexed with reference to the standard data as (220), (311), (400), (422), (511) and (440). These reflections indicate the presence of single phase cubic spinel structure without any impurity peak (311) plane has the maximum intensity which indicates the spinel phase. The crystallite size (D) of all the ferrite compositions was calculated using the Eq. (1) considering the (311) plane. The crystallite size was in the range of 37–42 nm as clear from Table 1.

Lattice parameter of the individual compositions was calculated using the relation 2 and was shown in Table 1. The calculated value of lattice parameter for Lithium ferrite was in good agreement with the standard data 8.33 Å from JCPDS No. 88-0671. It is clear that the calculated lattice parameter was 99.7% precise with a least error of 0.3%. It is observed that with an increase in Co composition from x=0.0–1.0 in $[Li_{0.5}Fe_{0.5}]_{1-x}Co_xFe_2O_4$, the lattice parameter has increased from 8.356 to 8.404 Å. This can be explained based on the ionic radii of the metal ions. The ionic radii of Li^+ ion (0.06 Å) and Fe^{3+} ion (0.64 Å) are smaller than that of the Co^{2+} ion (0.72 Å) which is acting as a dopant. That is, smaller ions are replaced by bigger ion, resulting in an increase in lattice parameter of synthesized individual ferrites with an increase in Co content from x=0.0 to 1.0. The variation of lattice parameter with Co composition is shown in Fig. 3.

X-ray density of the samples is calculated using the relation 3 and the values are recorded in the Table 1. It is observed that with an increase in Co (x) content, the X-ray density has also increased as evident from the Table 1 and Fig. 4. From the relation 3, it is clear that X-ray density depends on the molecular weight of the sample and lattice parameter. With the increase in Co content in $[Li_{0.5}Fe_{0.5}]_{1-x}Co_xFe_2O_4$ferrite system, the molecular weight of the sample is increased and the lattice parameter has also increased. The increase in X-ray density with the increase in Co content in the present ferrite system is because the increase in mass is more than the increase in volume of the unit cell. Similar behavior in the variation of lattice parameter and X-ray density with Co content was observed for cobalt substituted lithium ferrites synthesized by conventional ceramic technique as reported by Song et al. [19].

Volume of the unit cell is calculated from the relation 4 which depends on lattice parameter. It is observed that with an increase in Co content (x), the lattice parameter has increased. Hence there

Table 1
Crystallite size (D), Lattice parameter (a), X-ray density (d_x) and Volume of the unit cell (V) of $[Li_{0.5}Fe_{0.5}]_{1-x}Co_xFe_2O_4$ nano ferrites where $x=0.0, 0.2, 0.4, 0.6, 0.8, 1.0$.

Cr content	Ferrite composition	Molecular weight	Crystallite size-D (nm)	Lattice parameter-a (Å)	X-ray density-d_x (gm/cc)	Volume of the unit cell-V (Cm^3)
$X=0.0$	$Li_{0.5}Fe_{2.5}O_4$	207.079	41.90	8.356	4.713	583.44
$X=0.2$	$Li_{0.4}Co_{0.2}Fe_{2.4}O_4$	212.587	43.01	8.370	4.815	586.38
$X=0.4$	$Li_{0.3}Co_{0.4}Fe_{2.3}O_4$	218.095	38.44	8.375	4.931	587.43
$X=0.6$	$Li_{0.2}Co_{0.6}Fe_{2.2}O_4$	223.603	37.57	8.386	5.035	589.75
$X=0.8$	$Li_{0.1}Co_{0.8}Fe_{2.1}O_4$	229.111	37.06	8.395	5.144	591.65
$X=1.0$	$CoFe_2O_4$	234.619	36.90	8.404	5.250	593.55

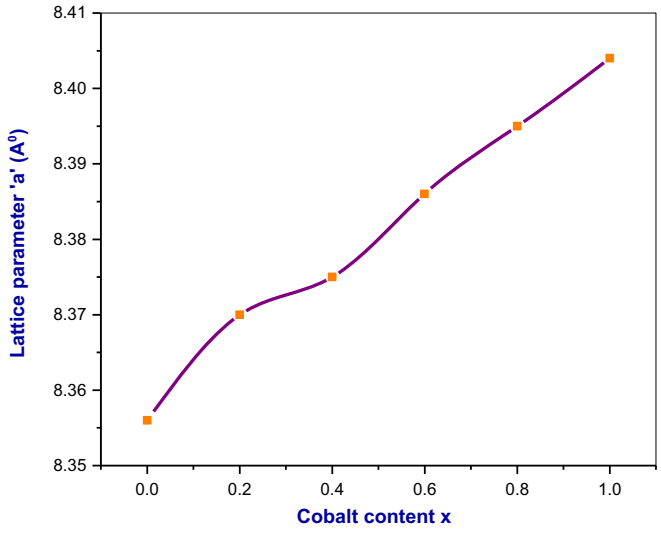

Fig. 3. Variation of lattice parameter with cobalt content for $[Li_{0.5}Fe_{0.5}]_{1-x}Co_xFe_2O_4$ where $x=0.0, 0.2, 0.4, 0.6, 0.8, 1.0$.

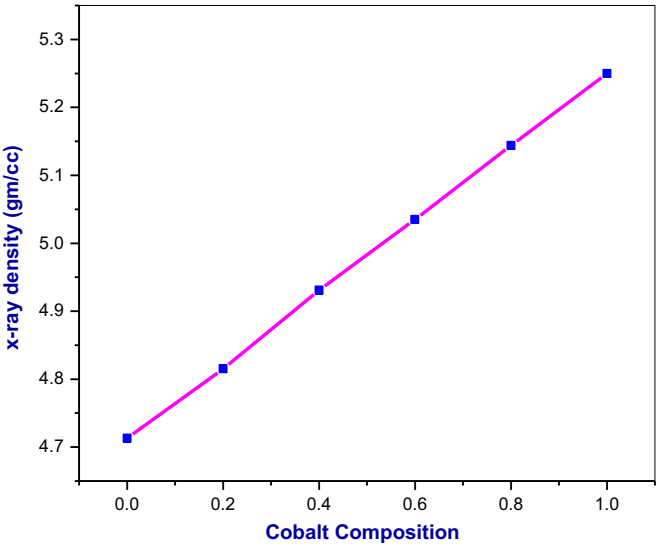

Fig. 4. Variation of X-ray density with cobalt content for $[Li_{0.5}Fe_{0.5}]_{1-x}Co_xFe_2O_4$ where $x=0.0, 0.2, 0.4, 0.6, 0.8, 1.0$.

is an increase in volume of the unit cell as clear from the Table 1 and Fig. 5.

5.2. Morphology by SEM

SEM images of the ferrite compositions under investigation were shown in Fig. 6. From the figure it is clear that the surface morphology of the particles is similar. The images represent large

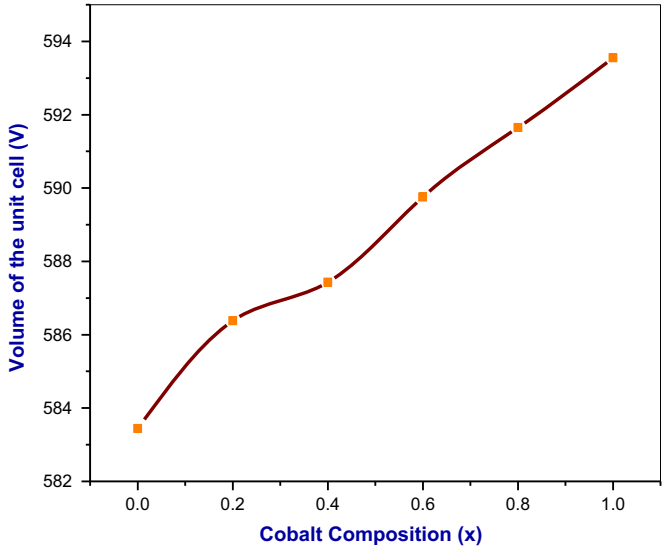

Fig. 5. Variation of volume of the unit cell with cobalt content for $[Li_{0.5}Fe_{0.5}]_{1-x}Co_xFe_2O_4$ where $x=0.0, 0.2, 0.4, 0.6, 0.8, 1.0$.

agglomeration of the nano particles of the ferrite samples where the distribution of the grain size is broad and not uniform. Such broader particle size of the samples confirms the formation of mechanically activated nano sized particles. The particles experience a permanent magnetic moment that is proportional to their volume resulting in the agglomeration of particles. Magnetic properties of the nano particles were affected by the Agglomeration of the ferrite nano particles. Agglomeration of the ferrites makes different ferrites with different alignments to come close to each other. This results in an increase in magneto crystalline anisotropy [20].

5.3. FC–ZFC magnetization study of $[Li_{0.5}Fe_{0.5}]_{1-x}Co_xFe_2O_4$ with $x=0.8$ and 1.0

Among the prepared lithium-cobalt nano ferrites of all compositions, the samples with Cobalt content $x=0.8$ and $x=1.0$ have the crystallite size of 37.06 nm and 36.9 nm. Ferrites with Such low particle size are expected to show superparamagnetic behavior. This has motivated the author to investigate the superparamagnetic behavior of these samples by performing Zero Field Cooled (ZFC) and Field Cooled (FC) magnetization measurements using the Vibrating Sample Magnetometer. Superparamagnetism is a phenomenon in which the magnetic materials behave as paramagnetic materials below the Curie temperature, unlike the general transition of a magnetic material from ferromagnetic to paramagnetic above its Curie temperature.

In the ZFC process, the ferrite sample is cooled in the absence of magnetic field. Then, the temperature is gradually raised by

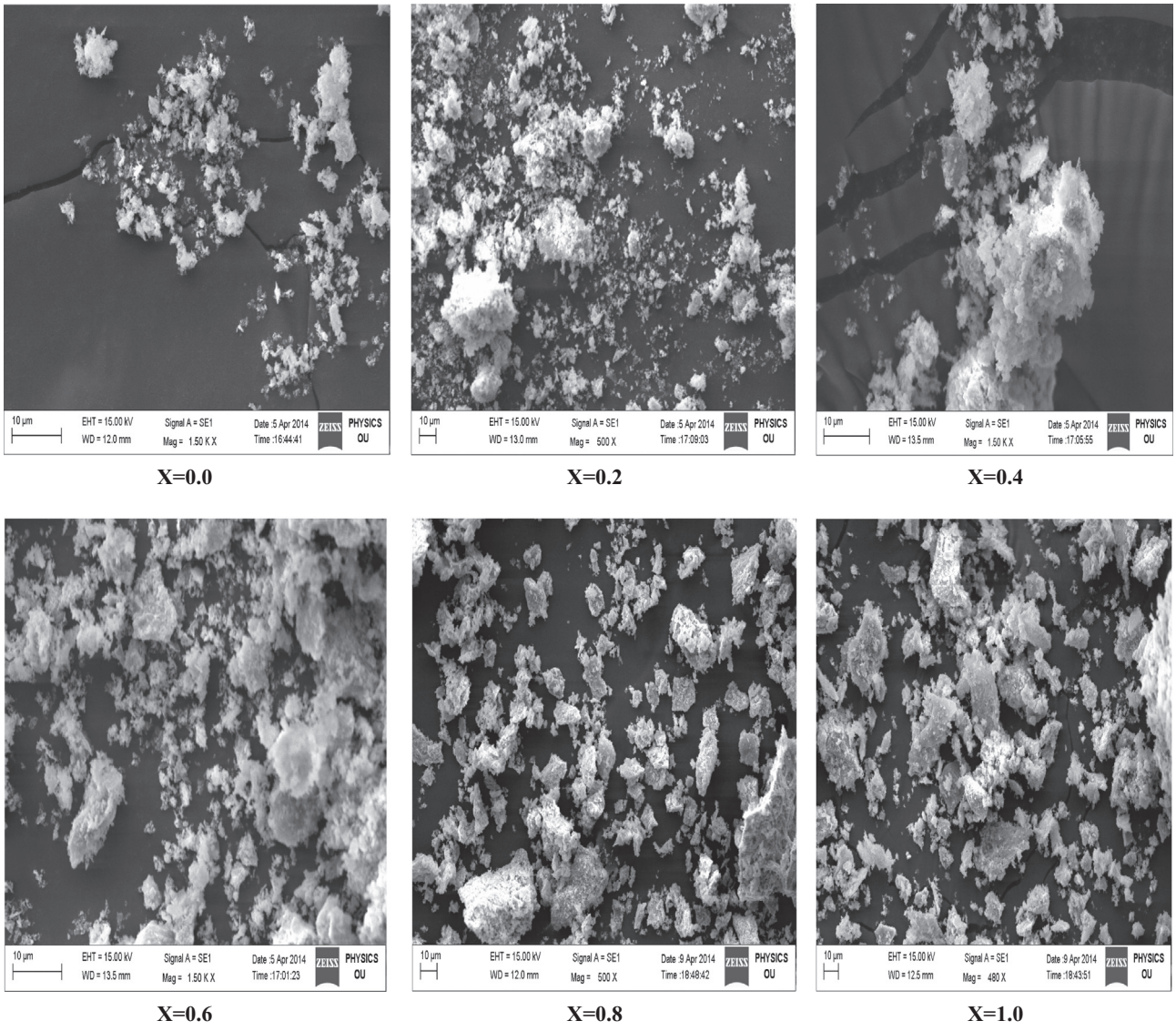

Fig. 6. SEM images for $[Li_{0.5}Fe_{0.5}]_{1-x}Co_xFe_2O_4$ where $x=0.0$, 0.2, 0.4, 0.6, 0.8, 1.0.

applying a moderate measuring field and the magnetization values (M) were recorded. In the FC process, the sample is cooled in the presence of a non-zero magnetic field and the same procedure is followed as in case of ZFC process.

Figs. 7 and 8 show the Magnetization–Temperature curves recorded in FC and ZFC modes for the samples $Li_{0.1}Co_{0.8}$ $Fe_{2.1}O_4$ and $CoFe_2O_4$ in an external magnetic field of 100 Oe and 1 KOe respectively.

In ZFC mode, the two ferrite samples under investigation i.e. $Li_{0.1}Co_{0.8}$ $Fe_{2.1}O_4$ and $CoFe_2O_4$ were cooled from 375 K down to 2 K in the absence of magnetic field. Then, a measuring field of 100 Oe and 1 KOe were applied and the magnetization measurements were made in the warming cycle. Whereas, in FC mode the samples were cooled from 375 K down to 2 K in the presence of the measuring field and then magnetization measurements were recorded as a function of rising temperature.

From the figures, it is clear that both the FC and ZFC magnetization decrease by decreasing the temperature for both the samples under two different applied fields (100 Oe and 1 KOe).

There exists a bifurcation between the FC and ZFC modes as evident from the figures owing to the magnetic relaxation nature of the nano particles and confirms their superparamagnetic nature. The temperature at which this bifurcation in the two modes is observed is defined as bifurcation temperature or blocking temperature (T_b). It is observed that the blocking temperature did not change with the increase in applied field, but shows a strong bifurcation in the FC and ZFC curves under higher applied field i.e. at 1 KOe, showing irreversibility of FC and ZFC magnetization curves. For both the samples the bifurcation or blocking temperature is observed at 350 K.

Figs. 9 and 10 show Magnetization Hysteresis curves for $Li_{0.1}Co_{0.8}$ $Fe_{2.1}O_4$ and $CoFe_2O_4$ samples at 5 K and 310 K. It is observed that the coercivity is more at lower temperature and it decreases with increase in temperature. The values of Coercivity (H_c) and remanence (M_r) were measured from the hysteresis curves and were recorded in Table 2. From the table it is clear that H_c and M_r values at 310 K for both the samples is very less which will approach zero at above room temperature. Zero coercivity and Zero remanence is the characteristic feature of the superparamagnetic behavior of the magnetic nano particles [21]. By comparing the FC–ZFC data and hysteresis curves data it is clear that below blocking temperature i.e. <350 K the material shows some hysteresis and hence behaves as ferromagnetic material. Above blocking temperature i.e. >350 K, hysteresis disappears

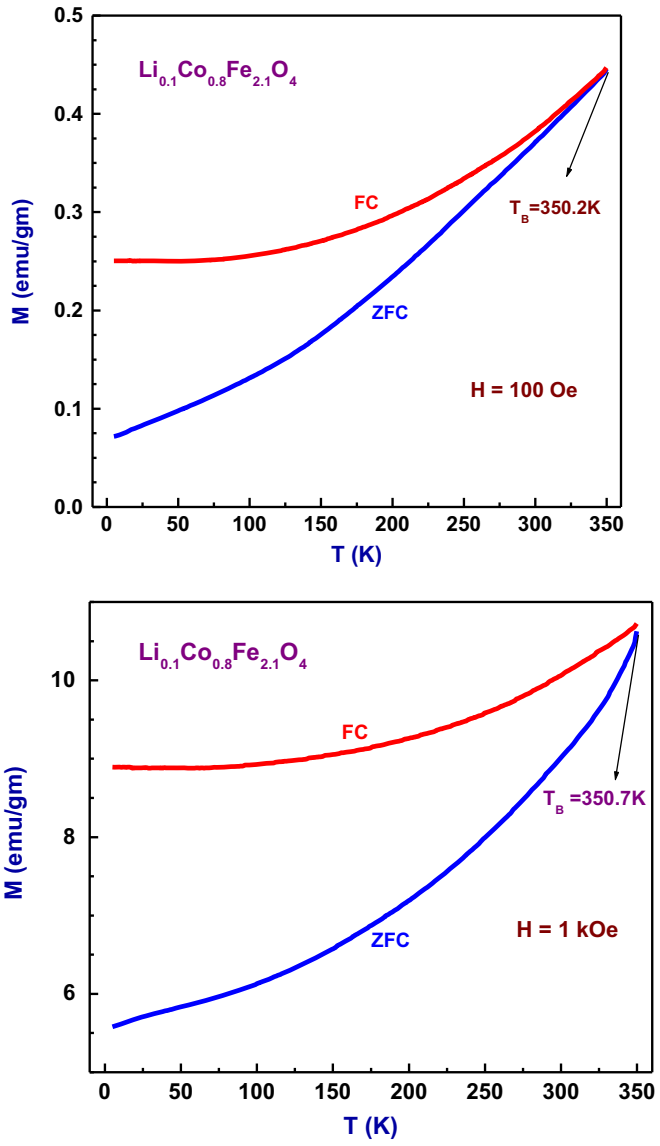

Fig. 7. Magnetization–Temperature curves recorded in FC and ZFC modes for the sample $Li_{0.1}Co_{0.8}$ $Fe_{2.1}O_4$ in an external magnetic field of 100 Oe and 1 KOe.

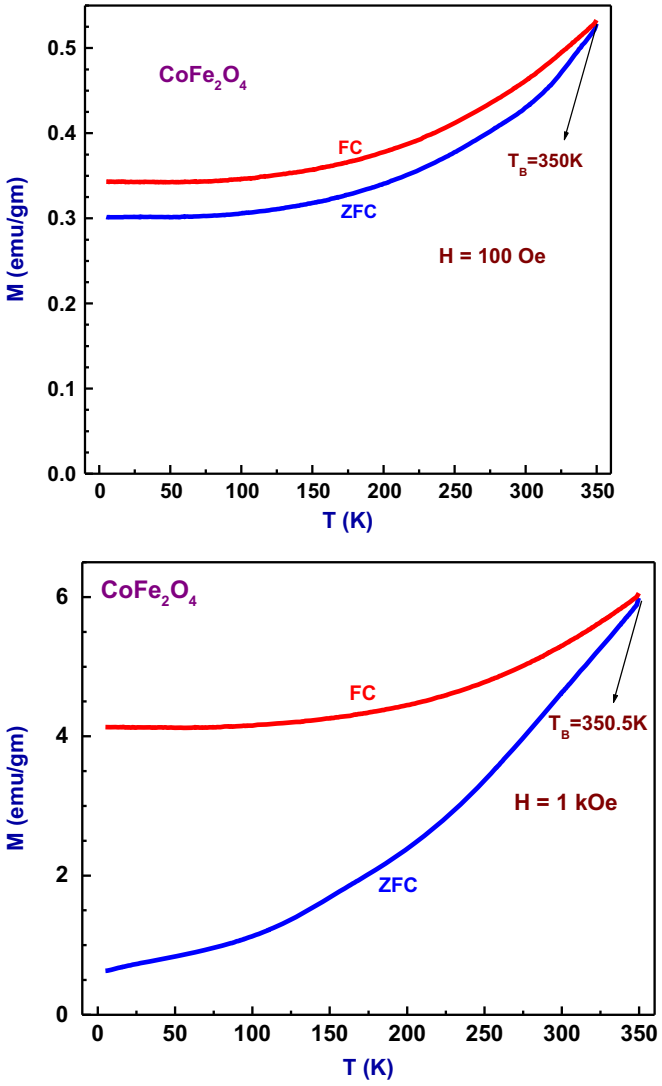

Fig. 8. Magnetization–Temperature curves recorded in FC and ZFC modes for the sample $CoFe_2O_4$ in an external magnetic field of 100 Oe and 1 KOe.

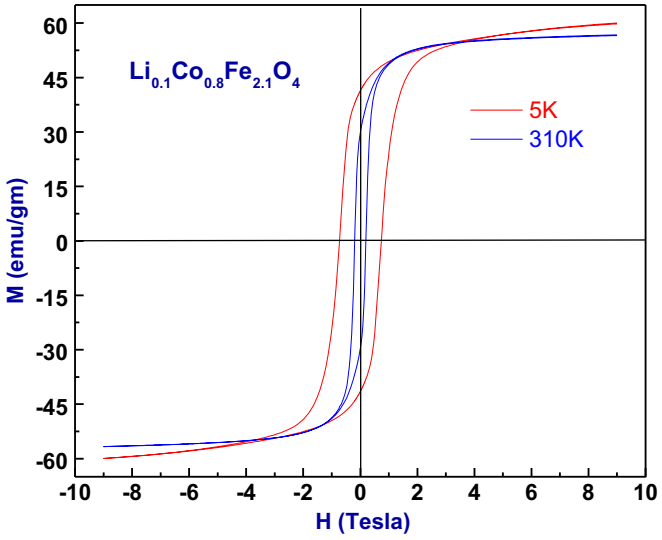

Fig. 9. Magnetization Hysteresis curves for $Li_{0.1}Co_{0.8}$ $Fe_{2.1}O_4$.

and the material behaves as superparamagnetic. Hence, Li–Co nano ferrites with superparamagnetic behavior are desirable for bio-medical applications.

6. Conclusion

Li–Co nano ferrites with the chemical composition $[Li_{0.5}Fe_{0.5}]_{1-x}Co_xFe_2O_4$ $x=0.0$, 0.2, 0.4, 0.6, 0.8, 1.0 were successfully prepared by Citrate gel auto-combustion technique with a crystallite size ranging from 37 to 42 nm. X-ray diffraction studies confirmed the formation of single phased cubic spinel structure of the ferrites without any impurity peak. The SEM analysis reveals the large agglomeration of the nano particles. Field cooled (FC) and Zero field cooled (ZFC) magnetization measurements on $Li_{0.1}Co_{0.8}$ $Fe_{2.1}O_4$ and $CoFe_2O_4$ nano ferrites under an applied field of 100 Oe and 1 KOe in the temperature range of 5–375 K have resulted the blocking temperature (T_b) at around 350 K i.e. above room temperature for both the ferrites. These two ferrites show ferromagnetic behavior below blocking temperature i.e. 350 K and show

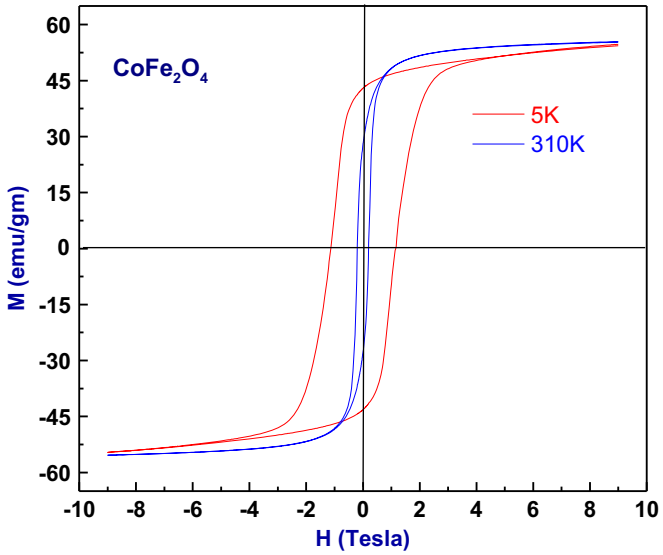

Fig. 10. Magnetization Hysteresis curves for $CoFe_2O_4$.

Table 2
Coercivity (H_c) and Remanence (M_r) of $Li_{0.1}$ $Co_{0.8}Fe_{2.1}O_4$ and $CoFe_2O_4$ from the Hysteresis curves.

Magnetic parameters	$Li_{0.1}$ $Co_{0.8}Fe_{2.1}O_4$		$CoFe_2O_4$	
	5 K	310 K	5 K	310 K
Coercivity (H_c)	0.74T	0.19T	1.11T	0.18T
Remanence (M_r) (emu/gm)	41.63	29.1	43.52	29.9

superparamagnetic behavior above 350 K. Hence, these ferrites are desirable for bio-medical applications.

Acknowledgment

The authors are very grateful to Prof. K. Venugopal Reddy, Head, Department of Physics, University College of Science, Osmania University for his support in carrying out the research work. Authors are thankful to Dr. V. Siruguri, Centre Director, UGC-DAE, Consortium for Scientific Research, Mumbai Centre and to Dr. P. D. Babu, Scientist, Mumbai centre for providing Low temperature Magnetic measurements. The authors are thankful to UGC, New Delhi for their financial assistance through Major Research Project.

References

[1] M. Raghasudha, D. Ravinder, P. Veerasomaiah, J. Magn. Magn. Mater. 355 (2014) 210.
[2] I. Soibam, S. Phanjoubam, C. Prakash, J. Magn. Magn. Mater. 321 (2009) 2779.
[3] A.M. Shaikh, C.M. Kanamadi, B.K. Chougule, Mater. Chem. Phys. 93 (2005) 548.
[4] S.A. Jadhav, Mater. Chem. Phys. 65 (2000) 120.
[5] N. Singh, A. Agarwal, S. Sanghi, P. Singh, J.Magn.Magn.Mater. 323 (2011) 486.
[6] A.M. Shaikh, S.S. Bellad, B.K. Chougule, J. Magn. Magn. Mater. 195 (1999) 384.
[7] K. Mohan, Y.C. Venudhar, J. Mater. Sci. Lett. 18 (1999) 13.
[8] S.S. Bellad, R.B. Pujar, B.K. Chougule, Mater. Chem. Phys. 52 (1998) 166.
[9] S.A. Mazen, F. Metawe, S.F. Mansour, J. Phys. D 30 (1997) 1799.
[10] S.A. Mazen, A. Elfalaky, A.Z. Mohamed, H.A. Hashem, Mater. Chem. Phys. 44 (1996) 293.
[11] C.S. Liu, W.B. Shu, M.J. Tung, M.Y. Ke, J. Appl. Phys. 67 (1990) 5506.
[12] S.C. Watawe, B.D. Sarwade, S.S. Bellad, B.D. Sutar, B.K. Chougule, J.Magn.Magn. Mater. 214 (2000) 55.
[13] M.C. Dimri, A. Verma, S.C. Kashyap, D.C. Dube, O.P. Thakur, C. Prakash, Mater. Sci. Eng. B 133 (2006) 42.
[14] L. Zhao, Y. Cui, H. Yang, L. Yu, W. Jin, S. Feng, Mater. Lett. 60 (2006) 104.
[15] R.S. Devan, Y.D. Kolekar, B.K. Chougule, J. Phys. Condens. Mater. 18 (2006) 9809.
[16] L. Yin, Q. Tai, Chin. Phys. 16 (2007) 3837.
[17] M. Raghasudha, D. Ravinder, P. Veerasomaiah, Adv. Mat. Lett. 4 (12) (2013) 910.
[18] M. Raghasudha, D. Ravinder, P. Veerasomaiah, Adv. Mat. Phy. Chem. 3 (2013) 89.
[19] J.M. Song, J.G. Koh, J. Magn. Magn. Mater. 152 (1996) 383.
[20] Sonal Singhal, Sheenu Jauhar, Jagdish Singh, Kailash Chandra, Sandeep Bansal, J. Mol. Stru. 1012 (2012) 182.
[21] C.P. Bean, I.S. Jacobs, Appl. Phys. 27 (1956) 1448.